Progress In Electromagnetics Research C, Vol. 104, 115–128, 2020

Analysis and Design of Two-Slot Antennas for Wireless Communication Applications

Khalil H. Sayidmarie* and Karam M. Younus

Abstract—This paper presents the design and investigation of array antennas formed of two narrow rectangular slots. Two approaches for feeding the two slots by microstrip lines are investigated as well as the influence of changing the distance between the slots on the radiation pattern. The two slots are etched on one side of the substrate, while the feed network is placed on the other side. Two designs, depending on the feeding approach, are presented. In the first design, a simple T-shaped divider is used to feed the two slots, while the second design is based on a single microstrip line which feeds the two slots in series. Two antennas are for the first design, each with dimensions of $57.83 \times 41.3\,\text{mm}^2$, while those of the second design have dimensions of $83.45 \times 36.9\,\text{mm}^2$. The four proposed designs have been simulated and optimized using Computer Simulation Technology (CST-MWS) simulation program. Prototypes were fabricated and tested to verify the designs. The four antennas achieved $-10\,\text{dB}$ impedance bandwidths between 8.6% and 9.4%, while the gain values were between 4.7 dB and 5.7 dB. The comparisons between the fabricated and simulated antennas considered the reflection coefficient and radiation pattern showing good agreement.

1. INTRODUCTION

The exponentially increasing applications and uses of wireless communications have led to design various antennas to work at various bands of the lower spectrum. With the use of mobile handsets and other portable communication devices, the need for small antennas has increased. When achieving small antennas, the idea of deploying small arrays of a few elements has attracted increasing interest.

One of the early examples of employing microstrip slots as a radiating aperture dates back to the use of the cavity-backed array antenna [1]. Various types of slot antennas have been designed to work in many bands of wireless systems [2]. Slot antenna, with the advantages of compact size, wide bandwidth, the possibility of flush-mounting, and easy integration with other devices, is a good candidate for portable and wireless systems [3, 4].

A slot with its enclosed electric field is an equivalent version to the dipole carrying a current; however, the feeding of the slot looks easier and more flexible. A slot-antenna fed by a microstrip line has been presented in [4], where the slot has a square shape and fed by a microstrip line with a tuning stub having a fork-shape to enhance the bandwidth. A low-profile slot antenna based on a quarter-wavelength microstrip feeding line has been illustrated in [5]. A new design for a merging ($\lambda/4$) slot antenna with a ($\lambda/4$) monopole has been reported in [6]. In [7], the author presented a new concept to excite slot antennas. Further investigations to enhance the bandwidth of a slot antenna were presented in [8, 9] by using different slots such as L and inverted T shapes. The L-shaped slot has one of its end opened; thus, it resonates at a 1/4 wavelength. In [10], an antenna structure consisting of two groups of five straight slots having different lengths was presented. The antenna operates at five different frequencies in the range 2 to 7.5 GHz.

Received 3 May 2020, Accepted 16 July 2020, Scheduled 3 August 2020

* Corresponding author: Khalil Hassan Sayidmarie (kh.sayidmarie@gmail.com).

The authors are with the Department of Communication Engineering, College of Electronic Engineering, Ninevah University, Mosul, Iraq.

In [11], an integrated slot antenna for a mobile handset with multiband features was proposed. The rectangular and square-shaped slots were intensively used in various antenna designs, but some modifications at the ends of the rectangular slot were investigated to achieve miniaturization [12]. It is worthy of mentioning that most of the published designs of slot antennas have either considered a single slot or more than one slot of various sizes to achieve multiband operation as in [13]. In [14], a series-fed, two-slot array was developed by placing two rectangular patches on the other side of the substrate to reduce radiation into the half-space that they occupy. The MIMO antenna in [15] has two elements, where each one comprises a circular slot that joins the other two vertical and horizontal ones. The slot in the ground plane offers the possibility to design a dual-function slot antenna as in [16, 17]. In these recent papers, microwave and millimetre-wave antennas for 4G and 5G are integrated into a single slot for mobile handset applications. Moreover, a single-slot antenna can be operated at more than one frequency by placing a PIN diode switch across the slot [18]. While two antennas were integrated into one slot, two slots were employed in a single mobile handset to furnish two bands that cover many wireless applications [19]. However, the design in [7] has presented an array of narrow rectangular slots. The effect of the distance between the slots on the feeding and radiated pattern was not studied.

This paper proposes an array antenna formed of two narrow rectangular slots, where two approaches for feeding the slots are investigated as well as the influence of the distance between the slots on the radiation pattern. Section 2 presents the design rules and characterization of the radiating slot. Then, the four designed antennas are presented in Sections 3 and 4 where simulated and experimental results are compared. The obtained conclusions are listed in Section 5.

2. ANTENNA DESIGN

The proposed slot antennas have been designed to operate at the (3.5 GHz) frequency for the WiMAX applications. Each antenna comprises two narrow rectangular slots fed by a microstrip line. The slots are etched on one side of the substrate while the feed network is printed on the other side of the substrate, as shown in Figure 1. The slot and its feeding with the microstrip line are described as follows.

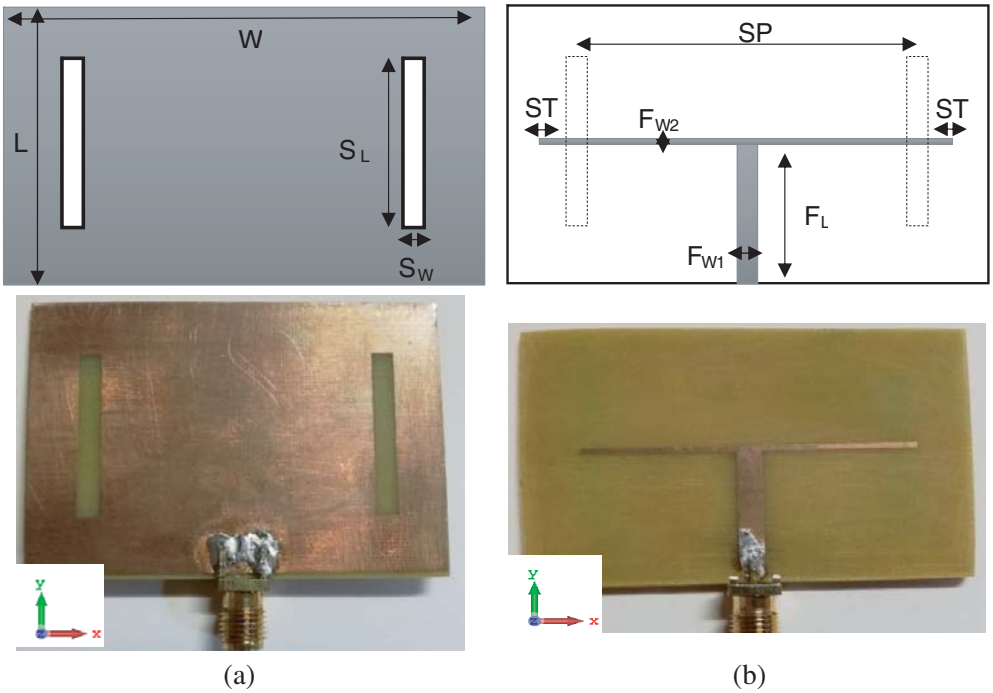

Figure 1. Geometry of the proposed Antenna-1 (Schematic and fabricated antenna). (a) Front-view (Slots-side). (b) Back-view (Feed-network with equal branches).

The effective wavelength in the slot and for the microstrip line can be found as follows [20]:

$$\varepsilon_e = \frac{\varepsilon_r + 1}{2} + \frac{\varepsilon_r - 1}{2}\left(1 + 12\frac{h}{Sw}\right)^{-0.5} \tag{1}$$

$$\lambda_e = \lambda_0/\sqrt{\varepsilon}_e \tag{2}$$

where λ_0 is the wavelength in free space, and λ_e is the effective wavelength inside the slot. ε_e is the effective dielectric constant, and ε_r is that for the substrate, while Sw and h are the width of the slot and the thickness of the substrate, respectively.

The width of the feedline was chosen to obtain a 50 Ω impedance (Z_o) of the feedline, where Z_o is given by [20]:

$$Z_0 = \begin{cases} \dfrac{60}{\sqrt{\varepsilon}_e}\ln\left[\dfrac{8h}{W_0} + \frac{W_0}{4h}\right] & \dfrac{W_0}{h} \le 1 \\ \sqrt{\varepsilon}_e\left[\dfrac{W_0}{h} + 1.393 + 0.667\ln\left(\dfrac{W_0}{h} + 1.444\right)\right] & \dfrac{W_0}{h} > 1 \end{cases} \tag{3}$$

where W_0 is the width of the microstrip line. The above relation was also used in the design of the divider circuit for feeding the two slots. The antenna array is fed by a simple T-shaped network, as shown in Figure 1. The 50 Ω microstrip line is branched into two lines, each having a 100 Ω impedance line. Using Eq. (3), the width of the main microstrip line was 3.14 mm, while the width of each of the two branches was found to be 0.72 mm.

The electric field lines in the slots are normal to the slot sides, and the field magnitude varies sinusoidally along the slot. The electric field at the two sides of the slot tends to zero, thus for the resonating slot variation forms 1/2 effective wavelength ($\lambda_e/2$) along the slot.

The radiating slot resonates at frequency f when its length S_L is equal to an integer N multiple of half the effective wavelength λ_e [18]:

$$S_L = N \times \frac{\lambda_e}{2} = N \times \left(\frac{C}{2f \times \sqrt{\varepsilon}_e}\right) \tag{4}$$

The chosen substrate is the widely and commercially available FR-4 with a thickness $h = 1.6$ mm, relative permittivity $\varepsilon_r = 4.3$, and loss tangent 0.025. For 3.5 GHz, the wavelength $\lambda_0 = 85.65$ mm and $\varepsilon_e = 3.27$, thus $\lambda_e = 47.36$ mm.

The radiation principle of slot-antennas can be explained by Babinet's principle, which states that "*The slot could be treated like a strip dipole antenna*" [20]. Thus, the slot length has been designed to be $\lambda_e/2$ at the operating frequency, and then its length is varied to optimize the performance. The first proposed design labeled as Antenna-1, where the two parallel slots are fed by a conventional T-shaped feed network, as shown in Figure 1, has the dimensions shown in Table 1. The designed antenna is investigated by a parametric study to examine the effects of the slot length S_L and stub length S_T, on the antenna performance.

Table 1. Optimized dimensions of the First Design (Antenna-1 and Antenna-2).

Parameter	W	L	S_L	S_W	S_P	S_T	F_L	F_{W1}	F_{W2}
Value in (mm)	57.83	41.3	24.1	3.14	40.31	0.7	20.6	3.14	0.72

2.1. Effect of the Slot's Length (S_L)

Figure 2 shows the effect of varying the slot length on the reflection coefficient parameter (S_{11}). It is obvious that the resonance frequency decreases as the slot length is increased. The optimum slot length is found to be $S_L = 24.7$ mm, which achieves better matching and desired band. This value is within 4.3% from the $\lambda_e/2$ value predicted by Eqs. (1), (2), and (4).

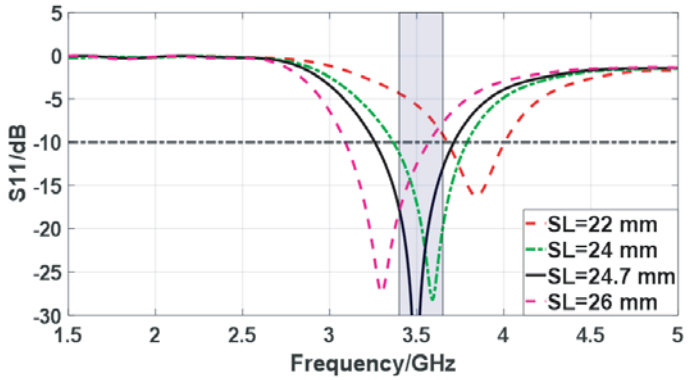

Figure 2. Variation of the S_{11} with frequency for various slot lengths S_L.

2.2. Effect of the Stub-Length (S_T)

The open-ended stub offers an impedance (Z_s) given as [18];

$$Z_s = -j \times Z_o \times \cot(\beta ST) \tag{5}$$

where Z_o is the impedance of the line feeding the slot and $\beta = 2\pi/\lambda_e$. Thus, by changing the stub length (S_T), a negative reactance is added at the point where the line meets the slot to enable matching. Figure 3 shows the effect of the stub length on matching, where the stub equal to 0.7 mm is found to give the best matching and the coverage of the desired band.

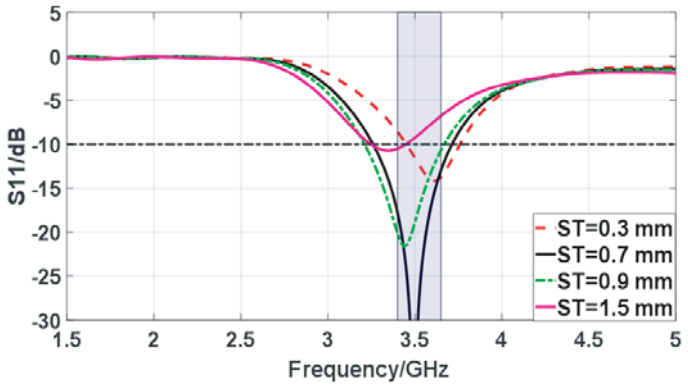

Figure 3. Variation of the S_{11} with frequency for various stub-lengths S_T.

Two feeding approaches are investigated here, where in the first one, the two slots are fed in parallel by a T-shaped corporate feeding network. In the second design, a single microstrip line feeds the two slots serially. For each design, two antennas have been presented to illustrate the effects of changing the distance between the slots on the radiation pattern.

3. FIRST DESIGN: (CENTERED T-SHAPED FEED)

In this design, the antenna is fed by a simple T-shaped network, as shown in Figure 1. The 50 Ω microstrip line is branched into two equal in length and having two 100 Ω impedance lines. The two 100 Ω branches feed the two slots, and each is extended by a length (S_T) beyond the slot to form a matching stub. The two slots are considered as a two-element antenna array. The T-shaped divider supplies each slot with the same level (magnitude) of excitation. However, the phase of the excitation is influenced by the length of the feed line and the orientation of the feed line with respect to the slot. Thus,

the spacing between the two elements plays a significant role in the shape of the radiation pattern. Two cases can be seen for the excitations of the two slots. The first one (Antenna-1) is when the phase-shift between the excitations of the two elements is zero. Thus, the antenna is in the broadside mode, and the pattern has one mainbeam. On the other hand, in Antenna-2, when the phases of the excitations of the two slots are different by $\lambda/2$ (*out-of-Phase*), the pattern will have a sharp-null perpendicular to the array plane, producing two lobes. The two cases are explained in the following.

3.1. Antenna-1: (Feeding with Branches of Equal-Lengths)

In this design, two slots are fed by branches of equal lengths, as shown in Figure 1(b). In this design, the spacing between the two slots is optimized to be 40.31 mm, which is about one effective wavelength (λ_e), or it is equal to $0.47\lambda_o$. Figure 4 illustrates the electric field across the two slots when they are fed by two branches of equal lengths (see Figure 1(b)). The electric field vectors in the two slots are in opposite directions, hence, in the far-field, the contributions of the two slots are phase-shifted by 180° in the normal direction to the antenna. This results in a null in the radiation pattern in the normal direction to the antenna, as shown in Figure 5. The 3D radiation pattern has 4.7 dBi gain, and the same figure shows good agreement between the measured and simulated patterns. The pattern is characterized by four lobes in the XZ-plane. The null in the normal direction to the antenna (Z-axis) is because the E-fields in the two slots are in opposite directions.

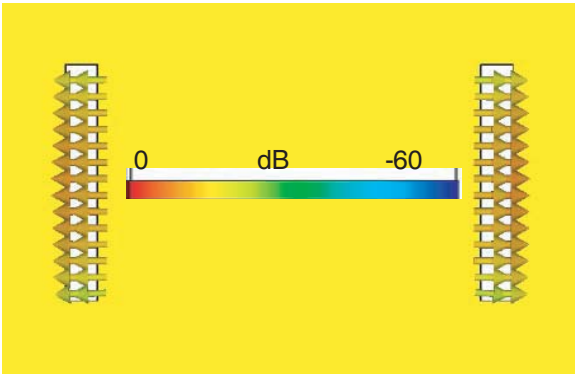

Figure 4. The E-field within the two slots when they are fed by two branches of equal lengths (Antenna-1).

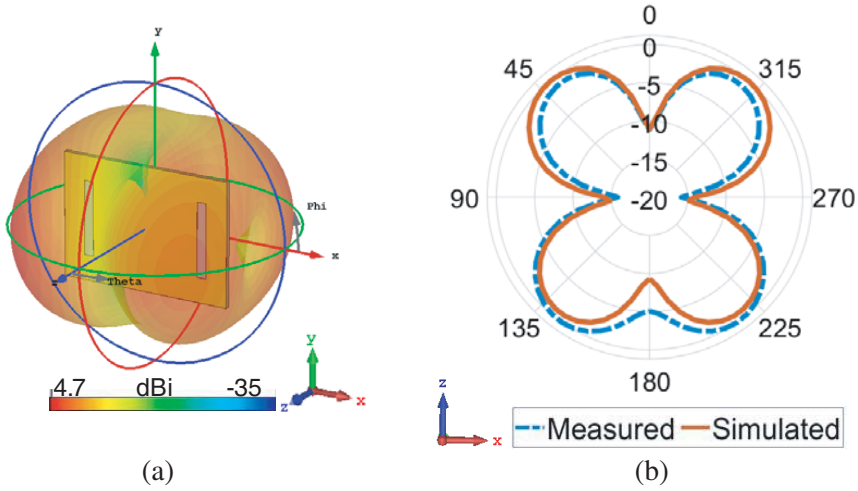

(a) (b)

Figure 5. Farfield radiation pattern of the proposed Antenna-1, when the two branches have equal lengths. (a) 3D transparent patterns. (b) Normalised 2D measured and simulated patterns (XZ-plane).

Figure 6 shows the reflection coefficient of the antenna (S_{11}) for both fabricated and simulated designs. It is clear that the antenna covers a bandwidth about 330 MHz (9.4%) and has an S_{11} less than (-25 dB) at the centre frequency of 3.5 GHz. Figure 7 shows the total gain and the radiation efficiency versus frequency for Antenna-1. The gain is about 4.7 dB, and the efficiency exceeds 90% across the operating band.

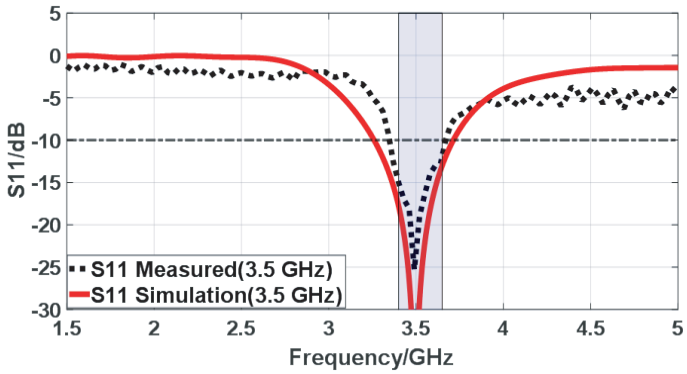

Figure 6. Simulated and measured S_{11} values versus frequency for Antenna-1.

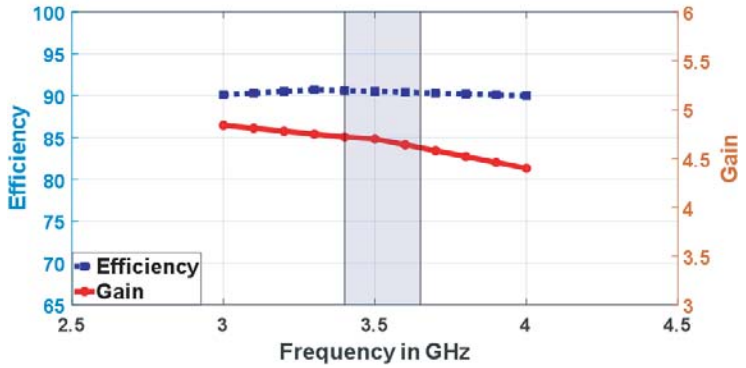

Figure 7. Antenna gain and efficiency versus frequency for Antenna-1.

3.2. Antenna-2: (Feeding with Branches of Unequal-Lengths)

In this case, the antenna was designed such that the electric field in the two slots should be in the same phase and that the antenna works in the broadside mode. This condition can be achieved by adding an extra length to one of the two branches of the feed network. Referring to the former case (Antenna-1), where there was a 180° phase shift between the two slots, thus an extra delay of $\lambda_e/2$ should be added to one of the two branches. The feed network was modified accordingly, as shown in Figure 8. In this design, the separation between the two slots was optimized so that the difference in the length of the two branches has been set to $2 \times L1 = 24.2\,\text{mm} \approx (\lambda_e/2)$. Figure 9 shows that the electric field vectors in the two slots are in the same phase; thus, they will furnish the broadside condition. Figure 10 shows the 3D radiation pattern, as well as a comparison between the simulated and measured patterns in the plane normal to the antenna (XZ-plane). The antenna has a maximum gain of 5.37 dB$_i$ in the normal direction to the antenna plane, thus achieving the broadside mode. The patterns show a conventional shape (like number 8) for the two-element broadside array. The measured pattern has some asymmetry due to some reflections in the measurement environment. The other feature in the patterns is that the field values in front and back sides of the antennas are slightly different, which can be attributed to the feed network lying on one side. Moreover, the slot at the ground plane side is in direct contact with air, while there is a substrate on the other side.

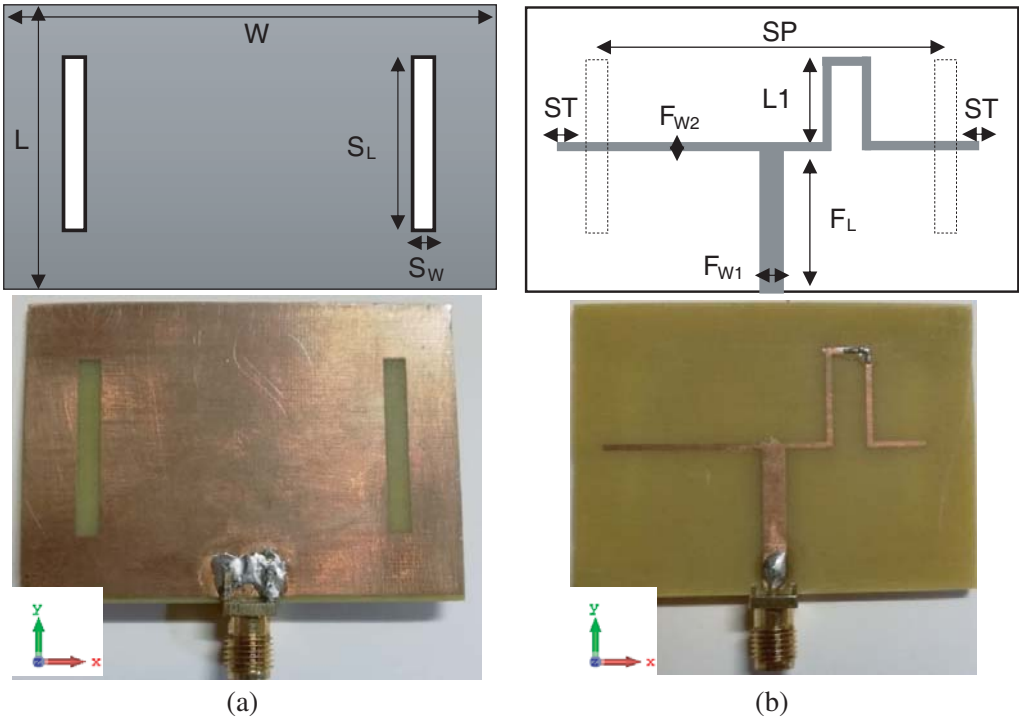

Figure 8. Geometry of the proposed Antenna-2, (schematic and fabricated antennas). (a) Front-view (slots-side). (b) Back-view (feed-network with unequal branches).

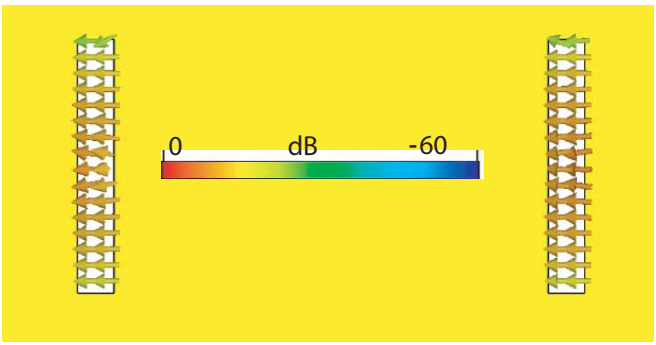

Figure 9. The E-field within the two slots when they are fed by two branches having $\lambda_e/2$ length difference.

Figure 11 shows the simulated and measured reflection coefficients of the antenna S_{11}. It is clear that the antenna covers a bandwidth more than 300 MHz and has an S_{11} better than -22 dB around the design frequency of 3.5 GHz. Figure 12 shows the total gain and the radiation efficiency versus frequency for Antenna-2. The gain is about 5.37 dB, and the efficiency is better than 91% across the operating band.

4. SECOND DESIGN: SERIES-FED SLOTS

In this design, the two slots are fed in series by a single microstrip line, as shown in Figure 13, Figure 18, and Table 2 which illustrate the antennas dimensions. The distance between the two slots influences the radiation pattern in two ways. The first is the delay along the feedline between the two slots, which controls the excitation phase of the second slot, and the other way is the typical effect of the phase shift

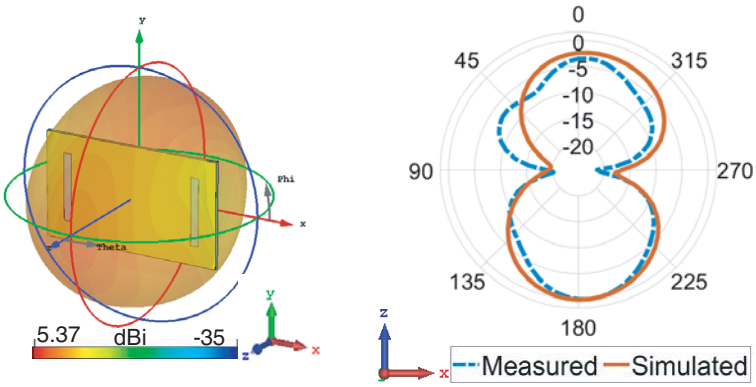

Figure 10. The far-field radiation pattern of the proposed Antenna-2 when the two branches have unequal lengths. (a) 3D Transparent patterns. (b) Normalised 2D measured and simulated patterns ($\varphi = 0°$).

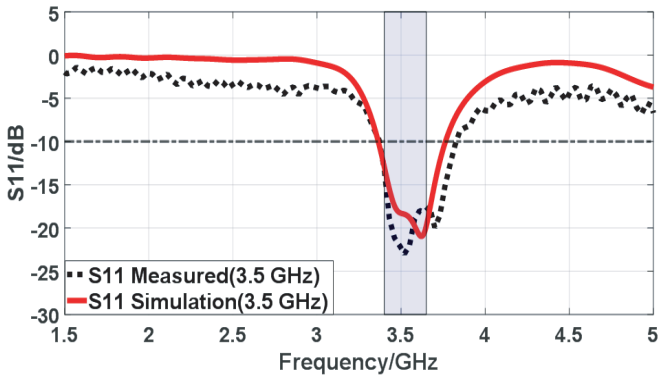

Figure 11. Simulated and measured S_{11} variation with frequency for the proposed Antenna-2.

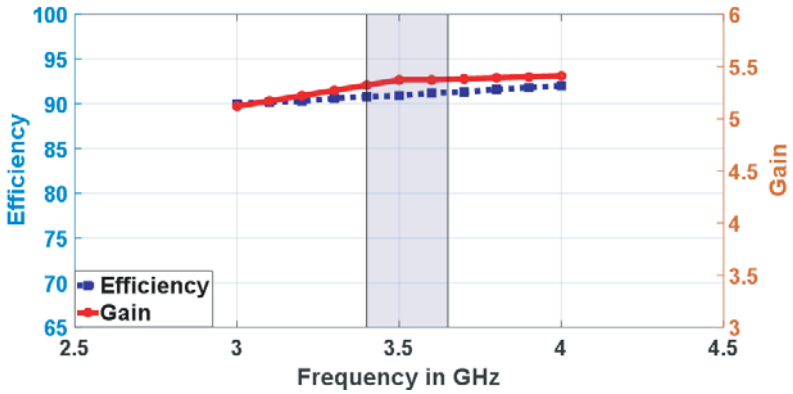

Figure 12. Antenna gain and efficiency versus frequency for Antenna-2.

between the two elements originating from their physical separation. Thus, as in the previous design, the two cases that influence the radiation pattern are considered in the following.

4.1. Antenna-3

In this case, the distance between the two slots was set equal to $\lambda_e/2$ as in Figure 13; thus, the two slots are fed by out of phase excitations, as it is evident from the plot of the electric field vectors in the

Table 2. Optimized dimensions of the Second Design (Antenna-3 and Antenna-4).

Parameter	W	S_P	L	S_L	S_W	S_T	F_L	F_W
Single-lobe *(Antenna-4)*	83.45	40.31	36.9	24.1	3.14	1.2	20	3.14
Two-lobes *(Antenna-3)*	63.3	20.15	36.9	24.1	3.14	1.2	20	3.14

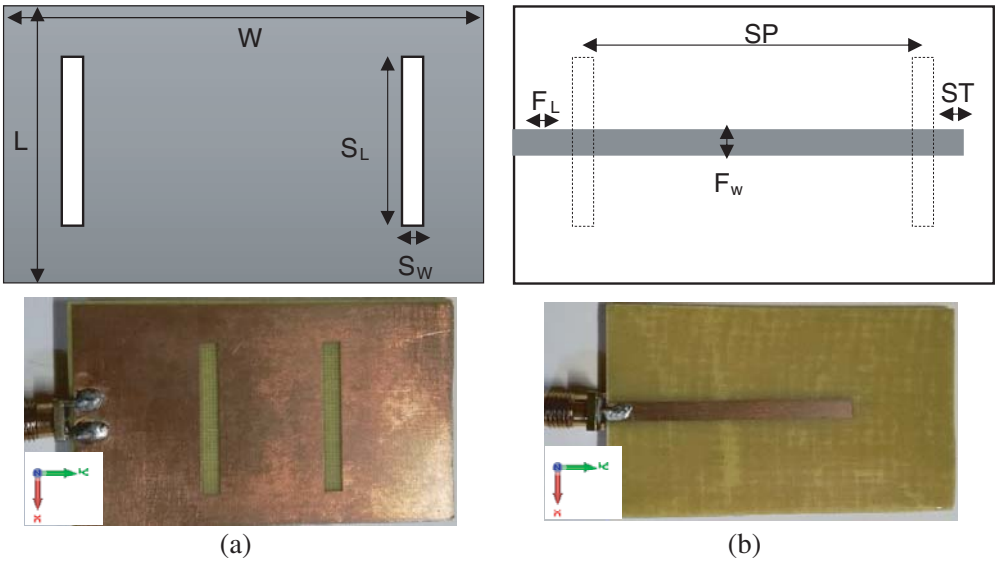

Figure 13. Geometry of the proposed antenna Antenna-3. (Schematic and fabricated antenna). (a) Front-view (slots-side). (b) Back-view (series seeding).

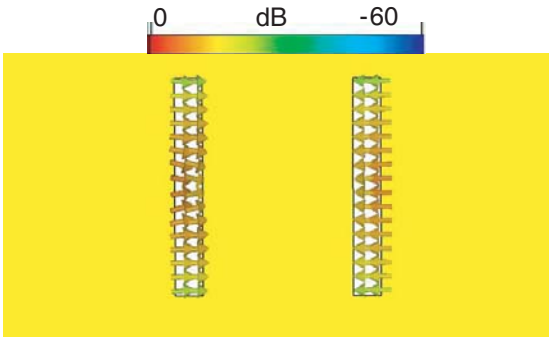

Figure 14. The E-field within the two slots when they are separated by $\lambda_e/2$.

two slots that are shown in Figure 14. The figure shows that the field vectors are in opposite directions. These excitations in the slots lead to a radiation pattern that possesses a null in the normal direction to the antenna, as shown in Figure 15, which illustrates the 3D radiation pattern. In this case, the spacing between the two slots was optimized to be 20.15 mm, which is $0.43\lambda_e$, where this spacing is equal to $0.24\lambda_o$. Thus, this two-element array has 1/4 wavelength separated elements that are excited in the antiphase case.

The antenna has a 5.67 dB gain, and the measured and simulated patterns are compared in Figure 15(b). The pattern has a null in the normal direction to the antenna plane (along the Z-axis)

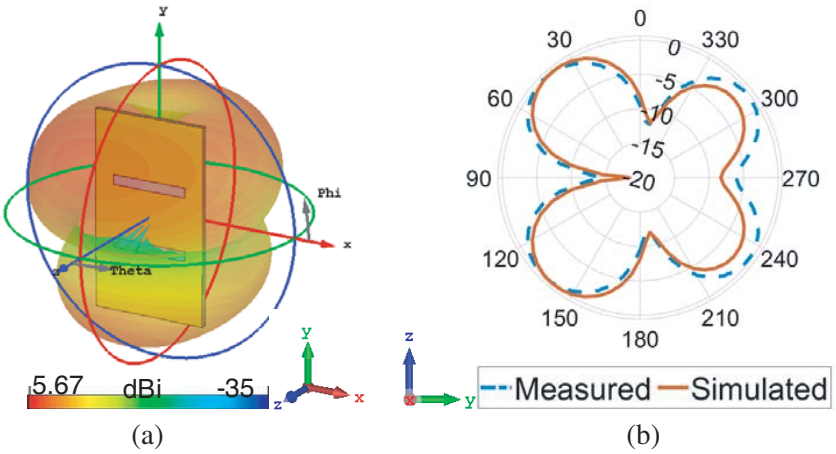

(a) (b)

Figure 15. The far-field radiation pattern of the proposed antenna for Antenna-3, when the two slots are separated by $\lambda_e/2$. (a) 3D Transparent patterns. (b) Normalised 2D measured and simulated patterns ($\varphi = 90°$).

due to the 180° phase shift between the two elements. The lobes are not symmetric with respect to the antenna normal especially for the measured pattern, due to the feed line and the antenna connector which is located at one side of the array.

Figure 16 shows the simulated and measured reflection coefficients (S_{11}). The antenna covers a bandwidth of more than 300 MHz and has an S_{11} better than −22 dB at the 3.5 GHz design frequency. Figure 17 shows the total gain and the radiation efficiency versus frequency for Antenna-3. The gain is about 5.67 dB, and the efficiency is around 90% across the operating band.

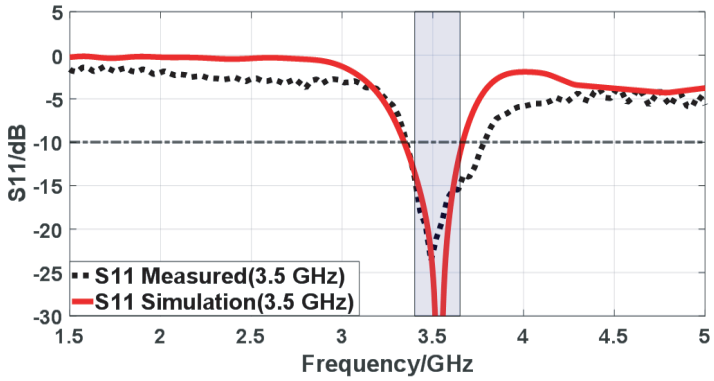

Figure 16. The simulated and measured S_{11} variation with frequency of the antenna Antenna-3.

4.2. Antenna-4

In this case, the distance between the two slots was set to one wavelength λ_e, as shown in Figure 18; thus, the two slots have in-phase excitations, as it is evident from the plot of the electric field vectors in the two slots that are shown in Figure 19. The figure shows field vectors in the same directions. For this design, the spacing between the two slots was optimized to 40.31 mm, so that the antenna is matched across the desired band around the centre frequency of 3.5 GHz, as shown in Figure 20. Figure 20 shows the simulated and measured reflection coefficients (S_{11}) of the antenna. The antenna covers a bandwidth of more than 305 MHz and has an S_{11} better than −15 dB around 3.5 GHz.

In this design, the used element separation of 40.31 mm is about one effective wavelength λ_e, which is equivalent to $0.47\lambda_o$. These parameters are for a 2-element broadside array that should have a radiation

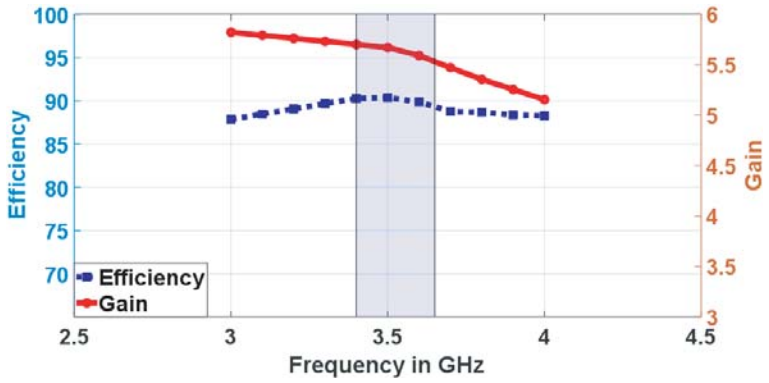

Figure 17. Antenna gain and efficiency versus frequency for Antenna-3.

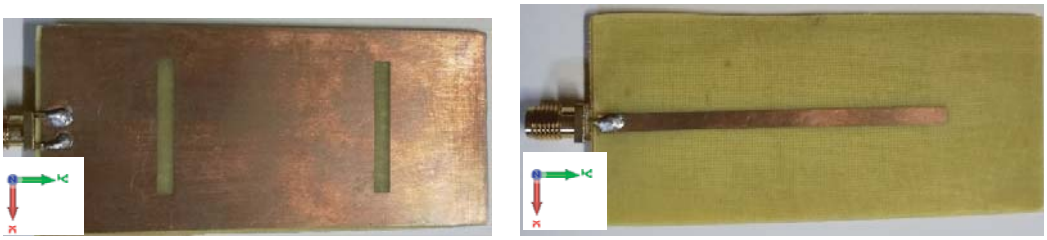

(a) (b)

Figure 18. Geometry of the proposed Antenna-4. (Schematic and fabricated antenna). (a) Front-view (slots-side). (b) Back-view (series feeding).

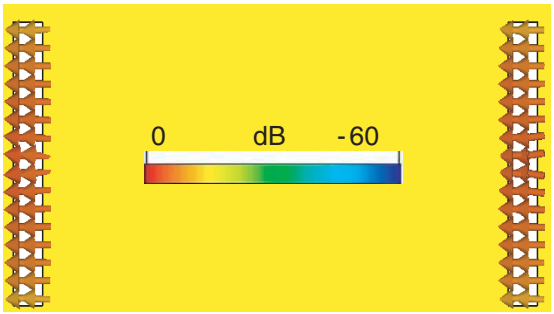

Figure 19. The E-field within the two slots when they are separated by λ_e.

pattern whose mainbeam is normal to the antenna plane, as shown in Figure 21, which illustrates the 3D radiation pattern. The antenna has achieved a maximum gain of 4.76 dB. The simulated and measured radiation patterns are compared in Figure 21(b). Referring to Figure 21, it can be seen that lobes are shifted from the array normal (Z-axis) by about 30°. The two slots are fed by a single microstrip line, and thus the actual phase shift between the two slots is not exactly zero. A Two-element array was modelled in MATLAB, where the elements are rectangular slots. The obtained results are shown in Figure 22 for the two cases of no phase shift and some phase shift between the elements. It is clear that the effect of the phase leads to scanning the main beam away from the array normal. Figure 23 shows the total gain and the radiation efficiency versus frequency for Antenna-4. The gain is about 4.76 dB, and the efficiency is better than 85% across the operating band.

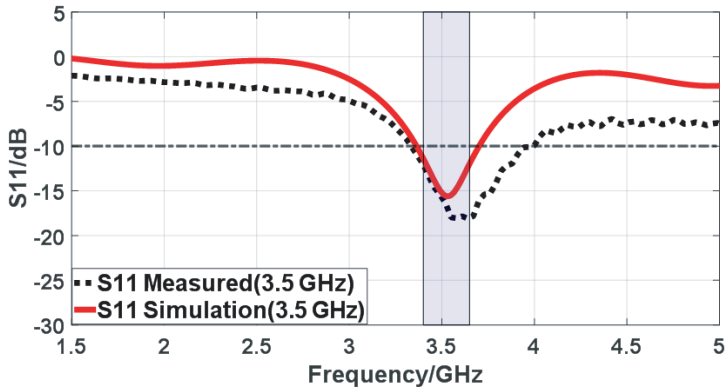

Figure 20. The simulated and measured S_{11} variation with frequency of Antenna-4.

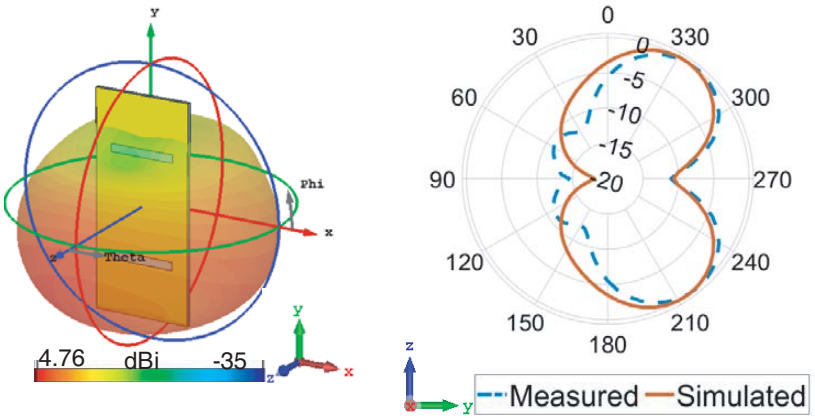

(a) (b)

Figure 21. The far-field pattern of the proposed Antenna-4 when the two slots are separated by λ_e. (a) 3D transparent patterns. (b) Normalised 2D measured and simulated patterns.

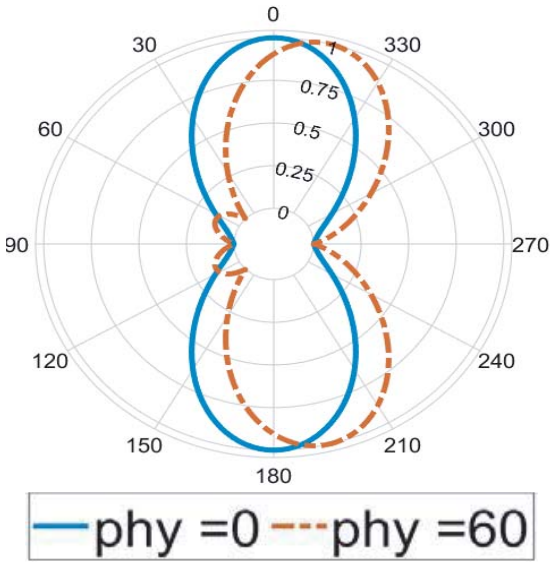

Figure 22. Simulated radiation patterns of a two-slot array, for various phase shift values ($phy(\varphi)$).

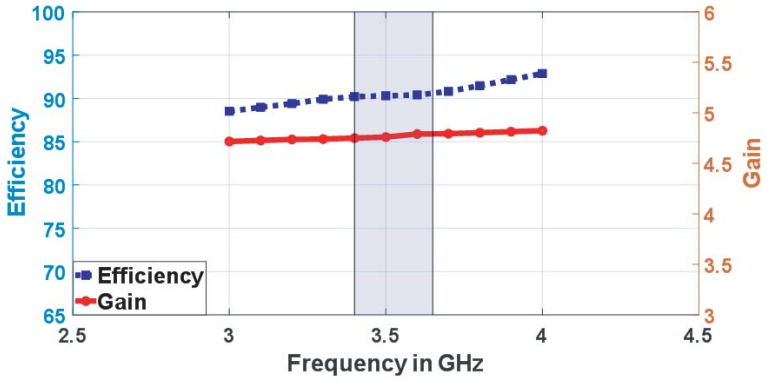

Figure 23. Antenna gain and efficiency versus frequency for Antenna-4.

5. CONCLUSION

An investigation of an array antenna formed of two narrow rectangular slots has been presented. Two approaches for feeding the two slots by microstrip lines are investigated as well as the influence of changing the distance between the slots on the radiation pattern. The first approach is achieved by using a T-shaped corporate network to feed the two slots, while the two slots are fed serially by a single microstrip line in the second approach. It has been found that the radiation pattern can be easily designed to produce either one main-beam or two lobes with a null perpendicular to the slot-plane by varying the length between the slots in terms of the effective wavelength. For each feeding approach, two designs have been presented to illustrate the effects of varying the distance between the two slots. To verify the proposed designs, prototypes of the four designed antennas have been fabricated and measured. The four antennas achieved -10 dB impedance bandwidths between 8.6% and 9.4%, while the gain values were between 4.7 dB and 5.7 dB. The array efficiency ranged from 85% to 90%. The comparison between the measured and simulated results showed excellent agreement in terms of reflection coefficient and radiation patterns.

REFERENCES

1. Li, R.-L., B. Pan, A. N. Traille, J. Papapolymerou, J. Laskar, and M. M. Tentzeris, "Development of a cavity-backed broadband circularly polarized slot/strip loop antenna with a simple feeding structure," *IEEE Transactions on Antennas and Propagation*, Vol. 56, No. 2, 312–318, Feb. 2008.
2. Xu, J. F., W. Hong, P. Chen, and K. Wu, "Design and implementation of low sidelobe substrate integrated waveguide longitudinal slot array antennas," *IET Microwaves, Antennas & Propagation*, Vol. 3, No. 5, 790–797, 2009.
3. Garg, R., P. Bhartia, I. Bahl, and A. Ittipiboon, *Microstrip Antenna Design Handbook*, Artech House, Norwood, MA, 2001.
4. Sze, J.-Y. and K.-L. Wong, "Bandwidth enhancement of a microstrip line-fed printed wide-slot antenna," *IEEE Transactions on Antennas and Propagation*, Vol. 49, 1020–1024, Jul. 2001.
5. Sharma, S. K., N. Jacob, and L. Shafai, "Low profile wide band slot antenna for wireless communications," *IEEE Antennas and Propagation Society International Symposium (IEEE Cat. No.02CH37313)*, Vol. 1, 390–393, San Antonio, TX, USA, 2002.
6. Ko, S. C. K. and R. D. Murch, "A diversity antenna for external mounting on wireless handsets," *IEEE Transactions on Antennas and Propagation*, Vol. 49, No. 5, 840–842, May 2001.
7. Nesic, A., "Slotted antenna array excited by a coplanar waveguide," *Electronics Letters*, Vol. 18, No. 6, 275–276, Mar. 18, 1982.
8. Sharma, S. K., L. Shafai, and N. Jacob, "Investigations of wideband microstrip slot antenna," *IEEE Transactions on Antennas and Propagation*, Vol. 52, No. 3, 865–872, Mar. 2004.

9. Latif, S. I., L. Shafai, and S. K. Sharma, "Bandwidth enhancement and size reduction of microstrip slot antennas," *IEEE Transactions on Antennas and Propagation*, Vol. 53, No. 3, 994–1003, Mar. 2005.
10. Gad, N. H. and M. Vidmar, "Design of a microstrip-fed printed-slot antenna using defected ground structures for multiband applications," *ACES Journal*, Vol. 33, No. 8, 854–860, Aug. 2018.
11. Zhong, J., R. M. Edwards, L. Ma, and X.-W. Sun, "Multiband slot antennas for metal back cover mobile handsets," *Progress In Electromagnetics Research Letters*, Vol. 39, 115–126, 2013.
12. Al-Nuaimi, M. K. T. and W. G. Whittow, "On the miniaturization of microstrip line-fed slot antenna using various slots," *IEEE Loughborough Antennas & Propagation Conference (LAPC)*, Loughborough, UK, 2011.
13. Sim, C.-Y.-D., Y.-W. Hsu, and C.-H. Chao, "Dual broadband slot antenna design for WLAN applications," *Microwave and Optical Technology Letters*, Vol. 56, No. 4, 983–988, Apr. 2014.
14. Rao, Q., T. A. Denidni, and R. H. Johnston, "A single-substrate microstrip-fed slot antenna array with reduced back radiation," *IEEE Antennas and Wireless Propagation Letters*, Vol. 3, 265–268, 2004.
15. Henderson, K. Q., S. I. Latif, G. Lazarou, S. K. Sharma, A. Tabbal, and S. Saial, "Dual-stub loaded microstrip line-fed multi-slot printed antenna for L TE bands," *2018 IEEE International Symposium on Antennas and Propagation & USNC/URSI National Radio Science Meeting*, 1743–1744, Boston, MA, 2018.
16. Ikram, M., E. A. Abbas, N. Nguyen-Trong, K. H. Sayidmarie, and A. Abbosh, "Integrated frequency-reconfigurable slot antenna and connected slot antenna array for 4G and 5G mobile handsets," *IEEE Transactions on Antennas and Propagation*, Vol. 67, No. 12, 7225–7233, Dec. 2019.
17. Ikram, M., N. Nguyen-Trong, and A. Abbosh, "Hybrid antenna using open-ended slot for integrated 4G/5G mobile application," *IEEE Antennas and Wireless Propagation Letters*, Vol. 19, No. 4, 710–714, Apr. 2020.
18. Younus, K. M. and K. H. Sayidmarie, "A tri-band frequency reconfigurable slot antenna for wireless applications," *ACES Journal — Applied Computational Electromagnetics Society*, Vol. 35, No. 2, 194–200, 2020.
19. Zhong, J., R. M. Edwards, L. Ma, and X. Sun, "Multiband slot antennas for metal back cover mobile handsets," *Progress In Electromagnetics Research Letters*, Vol. 39, 115–126, 2013.
20. Balanis, C. A., *Antenna Theory: Analysis and Design*, Chapter 14, 4th Edition, Wiley, 2016.